

# Swarm Intelligence Applied to 16-QAM DS-CDMA Multiuser Detectors

Bruno Augusto Angélico, Paul Jean Etienne Jeszensky, Taufik Abrão

**Abstract**—In this paper, the uplink direct sequence code division multiple access (DS-CDMA) multiuser detection problem (MUD) with 16-QAM modulation in flat Rayleigh channel with spatial diversity is studied into a heuristic perspective, named particle swarm optimization (PSO). A parameter optimization procedure for the PSO applied to MUD problem, regarding the acceleration coefficients ( $\phi_1$  and  $\phi_2$ ), is provided, which represents the major contribution of this paper. Simulation results show that, after convergence, the performance reached by the PSO-MUD is much better than the conventional detector, and somewhat close to the single user bound (SuB) for not so high system loading.

**Keywords**—16-QAM; DS-CDMA; multiuser detection; parameter optimization; PSO.

## I. INTRODUCTION

In a DS-CDMA system, a conventional detector (CD) may not provide a desirable quality of service, once the system capacity is strongly affected by multiple access interference (MAI), self-interference (SI), near-far effect (NFR) and fading [1], [2]. Multiuser detection emerged as a solution to overcome the MAI. The best performance is acquired by the optimum multiuser detection (OMUD), based on the log-likelihood function (LLF) [2]. In [3] it was demonstrated that multiuser detection problem results in a nondeterministic polynomial-time hard (NP-hard) problem. After the Verdu's revolutionary work, a great variety of suboptimal approaches have been proposed: from linear multiuser detectors [2], [4] to heuristic multiuser detectors [5], [6].

Examples of heuristic multiuser detection (HEUR-MUD) methods include: evolutionary programming (EP), specially the genetic algorithm (GA) [6], [7], particle swarm optimization (PSO) [8], [9], [10], [11] and, sometimes included in this classification, the deterministic local search (LS) methods [12], [13], which has been shown to present an very attractive performance  $\times$  complexity trade-off for low-order modulations.

High-order modulation in SISO or MIMO systems were previously addressed in [8], [9], [14]. In [14], PSO was applied to near-optimum asynchronous DS-CDMA multiuser detection problem under 16-QAM modulation and SISO multipath channels. Previous results on literature have shown that a simple local search optimization is enough to solve the MUD

problem with low-order modulation [13]. However for high-order modulation formats, the LS-MUD does not achieve good performances due to a lack of search diversity, whereas the PSO-MUD has been shown to be more efficient [14].

Recent works applying PSO to MUD usually assumes conventional values for PSO input parameters, such [15], or optimized values only for specific system and channel scenarios, such [10] for flat Rayleigh channel, [14] for multipath and high-order modulation, and [11] for multicarrier CDMA systems as well. This paper provides a simulated based parameter optimization of the PSO-MUD, in terms of PSO acceleration coefficients, applied to DS-CDMA systems in flat Rayleigh channels with 16-QAM modulations and spatial diversity of order two.

## II. SYSTEM MODEL

In this Section, a single-cell asynchronous multiple access DS-CDMA system model is described for Rayleigh channels and single or multiple antennas at the base station receiver. After describing the conventional detection approach with a maximum ratio combining (MRC) rule, the OMUD and the PSO-MUD are described. The model is generic enough to allow describing additive white Gaussian noise (AWGN) and flat Rayleigh channels, other modulation formats and single-antenna receiver.

### A. DS-CDMA

The base-band transmitted signal of the  $k$ th user is [16]

$$s_k(t) = \sqrt{\frac{\mathcal{E}_k}{T}} \sum_{i=-\infty}^{\infty} d_k^{(i)} g_k(t - iT), \quad (1)$$

where  $\mathcal{E}_k$  is the symbol energy, and  $T$  is the symbol duration. Each symbol  $d_k^{(i)}$ ,  $k = 1, \dots, K$  is taken independently and with equal probability from a complex alphabet set  $\mathcal{A}$  of cardinality  $M = 2^m$  in a squared constellation ( $m = 4$  for 16-QAM), i.e.,  $d_k^{(i)} \in \mathcal{A} \subset \mathbb{C}$ , where  $\mathbb{C}$  is the set of complex numbers. Gray mapping is assumed in the constellation. Fig. 1 sketches the  $K$  base-band DS-CDMA transmitters.

The normalized spreading sequence for the  $k$ -th user is given by

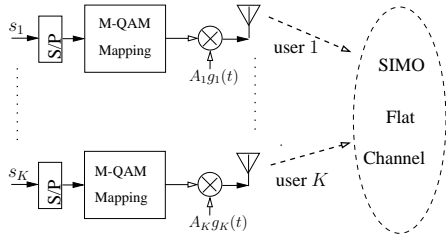
$$g_k(t) = \frac{1}{\sqrt{N}} \sum_{n=0}^{N-1} a_k(n) p(t - nT_c), \quad 0 \leq t \leq T, \quad (2)$$

where  $a_k(n)$  is a random sequence with  $N$  chips assuming the values  $\{\pm 1\}$ ,  $p(t)$  is the pulse shaping, assumed rectangular

Bruno Augusto Angélico, Federal University of Technology - Paraná (UTFPR), Cornélio Procopio, Brazil.

Paul Jean Etienne Jeszensky, Dept. of Telecomm. and Control Engineering, Escola Politécnica of the University of São Paulo, Brazil.

Taufik Abrão, Dept. of Electrical Engineering; State University of Londrina, Brazil.


 Fig. 1. Uplink base-band DS-CDMA transmission model with  $K$  users.

with unitary amplitude and duration  $T_c$ , with  $T_c$  being the chip interval. The processing gain is given by  $N = T/T_c$ .

The equivalent base-band received signal at  $q$ th receive antenna,  $q = 1, 2, \dots, Q$ , containing  $I$  symbols for each user in flat fading channel can be expressed by

$$r_q(t) = \sum_{i=0}^{I-1} \sum_{k=1}^K A_k d_k^{(i)} g_k(t - nT - \tau_{q,k}) h_{q,k}^{(i)} e^{j\varphi_{q,k}} + \eta_q(t), \quad (3)$$

with  $A_k = \sqrt{\frac{\mathcal{E}_k}{T}}$ ,  $\tau_{q,k}$  is the total delay for the signal of the  $k$ th user at  $q$ th receive antenna,  $e^{j\varphi_{q,k}}$  is the respective received phase carrier;  $\eta_q(t)$  is the additive white Gaussian noise with bilateral power spectral density equal to  $N_0/2$ , and  $h_{q,k}^{(i)}$  is the complex channel coefficient for the  $i$ th symbol, defined as

$$h_{q,k}^{(i)} = \gamma_{q,k}^{(i)} e^{j\theta_{q,k}^{(i)}}, \quad (4)$$

where the gain  $\gamma_{q,k}^{(i)}$  is a characterized by a Rayleigh distribution and the phase  $\theta_{q,k}^{(i)}$  by the uniform distribution  $\mathcal{U}[0, 2\pi]$ . A slow and frequency selective channel is assumed.

At the base station, the received signal is submitted to a matched filter bank (i.e., CD) per antenna of each user. Assuming perfect phase estimation (carrier phase), after despreading the resultant signal is given by

$$y_{q,k}^{(i)} = \frac{1}{T} \int_{nT}^{(i+1)T} r_q(t) g_k(t - \tau_{q,k}) dt = A_k h_{q,k}^{(i)} d_k^{(i)} + I_{q,k}^{(i)} + \tilde{\eta}_{q,k}^{(i)}. \quad (5)$$

The first term is the signal of interest, the second corresponds to the MAI, and the last one corresponds to the filtered AWGN. Considering a maximal ratio combining (MRC) rule with space diversity order equal to  $Q$  for each user, the  $M$ -level complex decision variable is given by

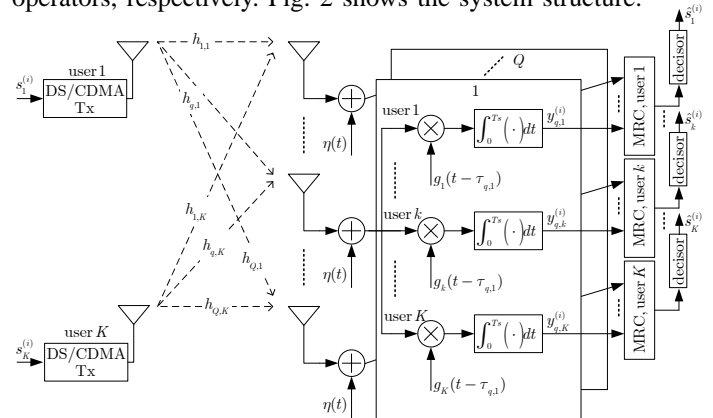
$$\zeta_k^{(i)} = \sum_{q=1}^Q y_{q,k}^{(i)} \cdot w_{q,k}^{(i)}, \quad k = 1, \dots, K \quad (6)$$

where the MRC weights  $w_{q,k}^{(i)} = \hat{\gamma}_{q,k}^{(i)} e^{-j\hat{\theta}_{q,k}^{(i)}}$ , with  $\hat{\gamma}_{q,k}^{(i)}$  and  $\hat{\theta}_{q,k}^{(i)}$  been a channel amplitude and phase estimation, respectively. After that, at each symbol interval, decisions are made on the in-phase and quadrature components of  $\zeta_k^{(i)}$  by scaling it into the constellation limits obtaining  $\xi_k^{(i)}$ , and choosing the complex symbol with minimum Euclidean distance regarding the scaled decision variable. Alternatively, this procedure can

be replaced by separate  $\sqrt{M}$ -level quantizers  $\text{qtz}$  acting on the in-phase and quadrature terms separately, such that

$$\hat{d}_k^{(i), \text{CD}} = \text{qtz}_{\mathcal{A}_{\text{real}}} \left( \Re \left\{ \xi_k^{(i)} \right\} \right) + j \text{qtz}_{\mathcal{A}_{\text{imag}}} \left( \Im \left\{ \xi_k^{(i)} \right\} \right), \quad (7)$$

for  $k = 1, \dots, K$ , and where  $\mathcal{A}_{\text{real}}$  and  $\mathcal{A}_{\text{imag}}$  is the real and imaginary value sets, respectively, from the complex alphabet set  $\mathcal{A}$ , and  $\Re\{\cdot\}$  and  $\Im\{\cdot\}$  representing the real and imaginary operators, respectively. Fig. 2 shows the system structure.


 Fig. 2. SIMO uplink base-band DS-CDMA system model with Conventional detector,  $K$  users and  $Q$  multiple receive antennas.

## B. Optimum Detection

The OMUD estimates the symbols for all  $K$  users by choosing the symbol combination associated with the minimal distance metric among all possible symbol combinations in the  $M = 2^m$  constellation points [2].

An one-shot approach is adopted, where a configuration with  $K$  asynchronous users,  $I$  symbols is equivalent to a synchronous scenario with  $KI$  virtual users [2]. Furthermore, in order to avoid handling complex-valued variables in high-order squared modulation formats, henceforward the alphabet set is re-arranged as  $\mathcal{A}_{\text{real}} = \mathcal{A}_{\text{imag}} = \mathcal{Y} \subset \mathbb{Z}$  of cardinality  $\sqrt{M}$ , i.e., 16-QAM ( $m = 4$ ),  $d_k^{(i)} \in \mathcal{Y} = \{\pm 1, \pm 3\}$ .

The OMUD is based on the maximum likelihood criterion that chooses the vector of symbols  $\underline{d}_p$ , formally defined in (13), which maximizes the metric

$$\underline{d}_p^{\text{opt}} = \arg \max_{\underline{d}_p \in \mathcal{Y}^{2KI}} \{ \Omega(\underline{d}_p) \}, \quad (8)$$

where, in a SIMO channel, the single-objective function is generally written as a combination of the LLFs from all receive antennas, given by

$$\Omega(\underline{d}_p) = \sum_{q=1}^Q \Omega_q(\underline{d}_p). \quad (9)$$

Generally, with  $K$  asynchronous users in a SIMO multipath Rayleigh channel, the LLF can be defined as a decoupled optimization problem with only real-valued variables, such that

$$\Omega_q(\underline{d}_p) = 2\underline{d}_p^T \mathbf{W}_q^T \underline{y}_q - \underline{d}_p^T \mathbf{W}_q \underline{\mathbf{R}} \mathbf{W}_q^T \underline{d}_p, \quad (10)$$

with definitions

$$\underline{y}_q := \begin{bmatrix} \Re\{\mathbf{y}_q\} \\ \Im\{\mathbf{y}_q\} \end{bmatrix}; \quad \mathbf{W}_q := \begin{bmatrix} \Re\{\mathbf{A}\mathbf{H}\} & -\Im\{\mathbf{A}\mathbf{H}\} \\ \Im\{\mathbf{A}\mathbf{H}\} & \Re\{\mathbf{A}\mathbf{H}\} \end{bmatrix};$$

$$\underline{\mathbf{d}}_p := \begin{bmatrix} \Re\{\mathbf{d}_p\} \\ \Im\{\mathbf{d}_p\} \end{bmatrix}; \quad \mathbf{R} := \begin{bmatrix} \mathbf{R} & \mathbf{0} \\ \mathbf{0} & \mathbf{R} \end{bmatrix}, \quad (11)$$

where  $\mathbf{y}_q \in \mathbb{R}^{2KI \times 1}$ ,  $\mathbf{W}_q \in \mathbb{R}^{2KI \times 2KI}$ ,  $\underline{\mathbf{d}}_p \in \mathcal{Y}^{2KI \times 1}$ ,  $\mathbf{R} \in \mathbb{R}^{2KI \times 2KI}$ . The vector  $\mathbf{d}_p \in \mathcal{Y}^{KI \times 1}$  in Eq. (11) is defined as

$$\mathbf{d}_p = \underbrace{[(d_1^{(1)} \dots d_1^{(1)}) \dots (d_K^{(1)} \dots d_K^{(1)})]}_{\text{times}} \dots \underbrace{[(d_1^{(I)} \dots d_1^{(I)}) \dots (d_K^{(I)} \dots d_K^{(I)})]}_{\text{times}} \dots \quad (12)$$

In addition, the  $\mathbf{y}_q \in \mathbb{C}^{KI \times 1}$  is the despread signal in Eq. (6) for a given  $q$ , in a vector notation, described as

$$\underline{\mathbf{y}}_q = \left[ (y_{q,1,1}^{(1)} \dots y_{q,1}^{(1)}) \dots (y_{q,K,1}^{(1)} \dots y_{q,K}^{(1)}) \dots \right. \\ \left. (y_{q,1,1}^{(I)} \dots y_{q,1}^{(I)}) \dots (y_{q,K,1}^{(I)} \dots y_{q,K}^{(I)}) \right] \quad (13)$$

Matrices  $\mathbf{H}$  and  $\mathbf{A}$  are the coefficients and amplitudes diagonal matrices, and  $\mathbf{R}$  represents the block-tridiagonal, block-Toeplitz cross-correlation matrix, composed by the submatrices  $\mathbf{R}[1]$  and  $\mathbf{R}[0]$ , such that [2]

$$\mathbf{R} = \begin{bmatrix} \mathbf{R}[0] & \mathbf{R}[1]^\top & \mathbf{0} & \dots & \mathbf{0} & \mathbf{0} \\ \mathbf{R}[1] & \mathbf{R}[0] & \mathbf{R}[1]^\top & \dots & \mathbf{0} & \mathbf{0} \\ \mathbf{0} & \mathbf{R}[1] & \mathbf{R}[0] & \dots & \mathbf{0} & \mathbf{0} \\ \dots & \dots & \dots & \dots & \dots & \dots \\ \mathbf{0} & \mathbf{0} & \mathbf{0} & \dots & \mathbf{R}[1] & \mathbf{R}[0] \end{bmatrix}, \quad (14)$$

with  $\mathbf{R}[0]$  and  $\mathbf{R}[1]$  being  $K$  matrices with elements

$$\underline{\rho}_{a,b}[0] = \begin{cases} 1, & \text{if } (k = u) \\ \rho_{k,u}^q, & \text{if } (k < u) \\ \rho_{u,k}^q, & \text{if } (k > u), \end{cases} \\ \underline{\rho}_{a,b}[1] = \begin{cases} 0, & \text{if } k \geq u \\ \rho_{u,k}^q, & \text{if } k < u \end{cases}. \quad (15)$$

The cross-correlation element between the  $k$ th user and  $u$ th user at  $q$ th receive antenna,  $\rho_{k,u}^q$ , is

$$\rho_{k,u}^q = \frac{1}{T} \int_0^T g_k(t - \tau_{q,k}) g_u(t - \tau_{q,u}) dt. \quad (16)$$

The evaluation in (8) considers  $I = 7$  symbols. ( $I$  must be, at least, equal to three). The vector  $\underline{\mathbf{d}}_p$  in (11) belongs to a discrete set with size depending on  $M$ ,  $K$ , and  $I$ . Hence, the optimization problem posed by (8) can be solved directly using a  $m$ -dimensional ( $m = \log_2 M$ ) search method. Therefore, the associated combinatorial problem strictly requires an exhaustive search in  $\mathcal{A}^{KI}$  possibilities of  $\mathbf{d}$ , or equivalently an exhaustive search in  $\mathcal{Y}^{2KI}$  possibilities of  $\underline{\mathbf{d}}_p$ . Hence, the maximum likelihood detector has a complexity that increases exponentially with  $m$ ,  $K$ , and  $I$ .

### C. Discrete Swarm Optimization Algorithm

A binary PSO [17] is considered in this paper. The particle selection for evolving is based on the highest fitness values obtained through (10) and (9). Accordingly, each candidate-vector defined like  $\mathbf{d}_i$  has its binary representation,  $\mathbf{b}_p[\mathbf{t}]$ , of size  $mKI$ , used for the velocity calculation, and the  $p$ th PSO

particle position at instant (iteration)  $\mathbf{t}$  is represented by the  $mKI \times 1$  binary vector

$$\mathbf{b}_p[\mathbf{t}] = [\mathbf{b}_p^1 \mathbf{b}_p^2 \dots \mathbf{b}_p^r \dots \mathbf{b}_p^{KI}]; \quad (17) \\ \mathbf{b}_p^r = [b_{p,1}^r \dots b_{p,\nu}^r \dots b_{p,m}^r]; \quad b_{p,\nu}^r \in \{0, 1\},$$

where each binary vector  $\mathbf{b}_p^r$  is associated with one  $d_k^{(i)}$  symbol in Eq. (13). Each particle has a velocity, which is calculated and updated according to

$$\mathbf{v}_p[\mathbf{t} + 1] = \omega \cdot \mathbf{v}_p[\mathbf{t}] + \\ + \phi_1 \cdot \mathbf{U}_{p_1}[\mathbf{t}] (\mathbf{b}_p^{\text{best}}[\mathbf{t}] - \mathbf{b}_p[\mathbf{t}]) + \\ + \phi_2 \cdot \mathbf{U}_{p_2}[\mathbf{t}] (\mathbf{b}_g^{\text{best}}[\mathbf{t}] - \mathbf{b}_p[\mathbf{t}]), \quad (18)$$

where  $\omega$  is the inertial weight;  $\mathbf{U}_{p_1}[\mathbf{t}]$  and  $\mathbf{U}_{p_2}[\mathbf{t}]$  are diagonal matrices with dimension  $mKI$ , whose elements are random variables with uniform distribution  $\mathcal{U} \in [0, 1]$ ;  $\mathbf{b}_g^{\text{best}}[\mathbf{t}]$  and  $\mathbf{b}_p^{\text{best}}[\mathbf{t}]$  are the best global position and the best local positions found until the  $\mathbf{t}$ th iteration, respectively;  $\phi_1$  and  $\phi_2$  are weight factors (acceleration coefficients) regarding the best individual and the best global positions, respectively.

For MUD optimization with binary representation, each element in  $\mathbf{b}_p[\mathbf{t}]$  in (18) just assumes “0” or “1” values. Hence, a discrete mode for the position choice is carried out inserting a probabilistic decision step based on threshold, depending on the velocity. Several functions have this characteristic, such as the sigmoid function [17]

$$S(v_{p,\nu}^r[\mathbf{t}]) = \frac{1}{1 + e^{-v_{p,\nu}^r[\mathbf{t}]}} \quad (19)$$

where  $v_{p,\nu}^r[\mathbf{t}]$  is the  $r$ th element of the  $p$ th particle velocity vector,  $\mathbf{v}_p^r = [v_{p,1}^r \dots v_{p,\nu}^r \dots v_{p,m}^r]$ , and the selection of the future particle position is obtained through the statement

$$\text{if } u_{p,\nu}^r[\mathbf{t}] < S(v_{p,\nu}^r[\mathbf{t}]), \quad b_{p,\nu}^r[\mathbf{t} + 1] = 1; \\ \text{otherwise,} \quad b_{p,\nu}^r[\mathbf{t} + 1] = 0, \quad (20)$$

where  $b_{p,\nu}^r[\mathbf{t}]$  is an element of  $\mathbf{b}_p[\mathbf{t}]$  (see Eq. (18)), and  $u_{p,\nu}^r[\mathbf{t}]$  is a random variable uniformly distributed,  $\mathcal{U} \in [0, 1]$ . After obtaining a new particle position  $\mathbf{b}_p[\mathbf{t} + 1]$ , it is mapped back into its correspondent symbol vector  $\mathbf{d}_p[\mathbf{t} + 1]$ , and further in the real form  $\underline{\mathbf{d}}_p[\mathbf{t} + 1]$ , for the evaluation of the objective function in (9).

In order to obtain further diversity for the search universe, the  $V_{\text{max}}$  factor is added to the PSO model, Eq. (18), being responsible for limiting the velocity in the range  $[\pm V_{\text{max}}]$ . The insertion of this factor in the velocity calculation enables the algorithm to escape from possible local optima. The likelihood of a bit change increases as the particle velocity crosses the limits established by  $[\pm V_{\text{max}}]$ , as shown in Tab. I.

TABELA I

MINIMUM BIT CHANGE PROBABILITY AS A FUNCTION OF $V_{\text{max}}$ .					
$V_{\text{max}}$	1	2	3	4	5
$1 - S(V_{\text{max}})$	0.269	0.119	0.047	0.018	0.007

Population size  $\mathcal{P}$  is typically in the range of 10 to 40 [18]. However, based on [10], it is set to

$$\mathcal{P} = 10 \left\lceil 0.3454 \left( \sqrt{\pi(mKI - 1)} + 2 \right) \right\rceil. \quad (21)$$

Algorithm 1 describes the pseudo-code of PSO.

**Algorithm 1** PSO Algorithm for the MUD Problem

**Input:**  $\mathbf{d}^{\text{CD}}$ ,  $\mathcal{P}$ ,  $G$ ,  $\omega$ ,  $\phi_1$ ,  $\phi_2$ ,  $V_{\max}$ ;     **Output:**  $\mathbf{d}^{\text{PSO}}$   
 begin  
 1. initialize first population:  $\mathbf{t} = 0$ ;  
     $\mathbf{B}[0] = \mathbf{b}^{\text{CD}} \cup \mathbf{B}$ , where  $\mathbf{B}$  contains  $(\mathcal{P}-1)$  particles randomly generated;  
     $\mathbf{b}_p^{\text{best}}[0] = \mathbf{b}_p[0]$  and  $\mathbf{b}_g^{\text{best}}[0] = \mathbf{b}^{\text{CD}}$ ;  
     $\mathbf{v}_p[0] = \mathbf{0}$ : null initial velocity;  
 2. while  $\mathbf{t} \leq G$   
    a. calculate  $\Omega(\mathbf{d}_p[\mathbf{t}])$ ,  $\forall \mathbf{b}_p[\mathbf{t}] \in \mathbf{B}[\mathbf{t}]$  using (9);  
    b. update velocity  $\mathbf{v}_p[\mathbf{t}]$ ,  $p = 1, \dots, \mathcal{P}$ , through (18);  
    c. update best positions:  
       for  $p = 1, \dots, \mathcal{P}$   
         if  $\Omega(\mathbf{d}_p[\mathbf{t}]) > \Omega(\mathbf{d}_p^{\text{best}}[\mathbf{t}])$ ,  $\mathbf{b}_p^{\text{best}}[\mathbf{t} + 1] \leftarrow \mathbf{b}_p[\mathbf{t}]$   
         else  $\mathbf{b}_p^{\text{best}}[\mathbf{t} + 1] \leftarrow \mathbf{b}_p^{\text{best}}[\mathbf{t}]$   
       end  
       if  $\exists \mathbf{b}_p[\mathbf{t}]$  such that  $[\Omega(\mathbf{d}_p[\mathbf{t}]) > \Omega(\mathbf{d}_g^{\text{best}}[\mathbf{t}]) \wedge$   
            $[\Omega(\mathbf{d}_p[\mathbf{t}]) \geq \Omega(\mathbf{d}_j[\mathbf{t}]), j \neq p],$   
            $\mathbf{b}_g^{\text{best}}[\mathbf{t} + 1] \leftarrow \mathbf{b}_p[\mathbf{t}]$   
           else  $\mathbf{b}_g^{\text{best}}[\mathbf{t} + 1] \leftarrow \mathbf{b}_g^{\text{best}}[\mathbf{t}]$   
    d. Evolve to a new swarm population  $\mathbf{B}[\mathbf{t} + 1]$ , using (20);  
    e. set  $\mathbf{t} = \mathbf{t} + 1$ .  
   end  
 3.  $\mathbf{b}^{\text{PSO}} = \mathbf{b}_g^{\text{best}}[G]$ ;  $\mathbf{d}^{\text{PSO}} \xrightarrow{\text{map}} \mathbf{d}^{\text{PSO}}$ .  
 end

-----  
 $\mathbf{d}^{\text{CD}}$ : CD output;  $\mathcal{P}$ : Population size;  $G$ : number of swarm iterations.  
 For each  $\mathbf{d}_p[\mathbf{t}]$  there is a  $\mathbf{b}_p[\mathbf{t}]$  associated.

## III. PSO-MUD PARAMETERS OPTIMIZATION

PSO-MUD parameters optimization is carried out using Monte Carlo simulation.

A first analysis of the PSO parameters gives raise to the following behaviors:  $\omega$  is responsible for creating an inertia of the particles, inducing them to keep the movement towards the last directions of their velocities;  $\phi_1$  aims to guide the particles to each individual best position, inserting diversification in the search;  $\phi_2$  leads all particles towards the best global position, hence intensifying the search and reducing the convergence time;  $V_{\max}$  inserts perturbation limits in the movement of the particles, allowing more or less diversification in the algorithm.

The optimization process for the initial velocity of the particles achieves similar results for three different conditions: null, random and CD output as initial velocity. Hence, it is adopted here, for simplicity, null initial velocity, i.e.,  $\mathbf{v}[0] = \mathbf{0}$ . The  $V_{\max}$  parameter was set to  $V_{\max} = 4$ .

A relatively larger value for  $\omega$  is helpful for global optimum, and lesser influenced by the best global and local positions, while a relatively smaller value for  $\omega$  is helpful for course convergence, i.e., smaller inertial weight encourages the local exploration [18], [19] as the particles are more attracted towards  $\mathbf{b}_p^{\text{best}}[\mathbf{t}]$  and  $\mathbf{b}_g^{\text{best}}[\mathbf{t}]$ .  $\omega$  achieves a good performance  $\times$  complexity trade-off (results not shown).

A special attention is given for  $\phi_1$  and  $\phi_2$  optimization in the next, since their values impact deeply in the PSO performance, also varying for each modulation. Fig. 3 shows the convergence curves for different values of  $\phi_1$  and  $\phi_2$ . The term  $\text{SER}_{\text{Avg}}$  represents the average symbol error rate.  $\phi_1 = 6$  and  $\phi_2 = 1$  are chosen.

For system with spatial diversity ( $Q > 1$  receive antennas), the same optima values were observed.

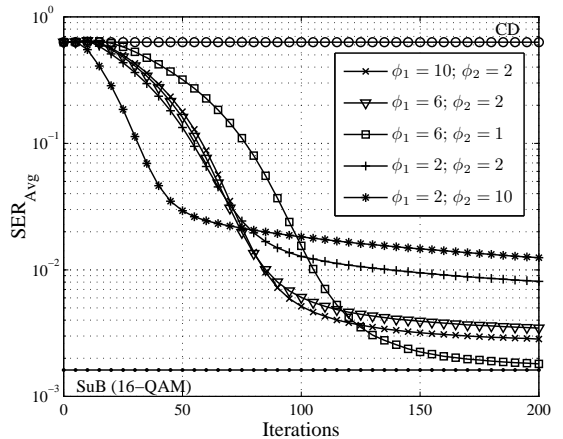


Fig. 3.  $\phi_1$  and  $\phi_2$  optimization under flat Rayleigh channels for 16-QAM modulation,  $E_b/N_0 = 30$  dB,  $K = 15$ ,  $\omega = 1$  and  $V_{\max} = 4$ .

## IV. NUMERICAL RESULTS WITH OPTIMIZED PARAMETERS

In this section, numerical performance results are obtained using Monte-Carlo simulations. The results are compared with theoretical single-user bound (SuB), according to Appendix A, since the OMUD computational complexity results prohibitive. The adopted PSO-MUD parameters, as well as system and channel conditions employed in Monte Carlo simulations are summarized in Tab. II.

TABELA II  
SYSTEM, CHANNEL AND PSO-MUD PARAMETERS FOR FADING CHANNELS PERFORMANCE ANALYSIS.

Parameter	Adopted Values
<i>DS-CDMA System</i>	
# Rx antennas	$Q = 1, 2$
Spreading Sequences modulation	Random, $N = 31$ 16-QAM
# mobile users	$K \in [5; 25]$
Received SNR	$E_b/N_0 \in [0; 30]$ dB
<i>PSO-MUD Parameters</i>	
Population size, $\mathcal{P}$	Eq. (21)
acceleration coefficients	$\phi_1 = 6; \phi_2 = 1$
inertia weight	$\omega = 1$
Maximal velocity	$V_{\max} = 4$
<i>Flat Rayleigh Channel</i>	
Channel state info. (CSI)	perfectly known at Rx coefficient error estimates

Fig. 4 shows convergence performance of the the PSO-MUD for low system loading<sup>1</sup>. It can be seen that, in this case, 40 to 50 iterations are enough for achieving a good convergence. Spatial diversity with  $Q = 2$  antennas is considered and compared to the case of  $Q = 1$  antenna.

Fig. 5 shows the SER performance as a function of the SNR. It is worth pointing out that the performance of the PSO-MUD under medium system loading ( $K = 15$ ) reaches the SuB for  $Q = 1$  and  $Q = 2$ , for all evaluated SNR range.

<sup>1</sup>In a CDMA scheme, the system loading is defined as  $K/N$ , where  $N$  represents the processing gain, which is assumed  $N = 31$  in this work.

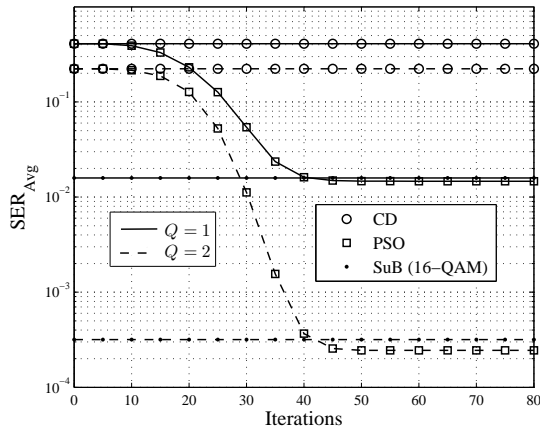


Fig. 4. Convergence of PSO-MuD under flat Rayleigh channel,  $E_b/N_0 = 20$  dB, and  $K = 6$  users with 16-QAM modulation.

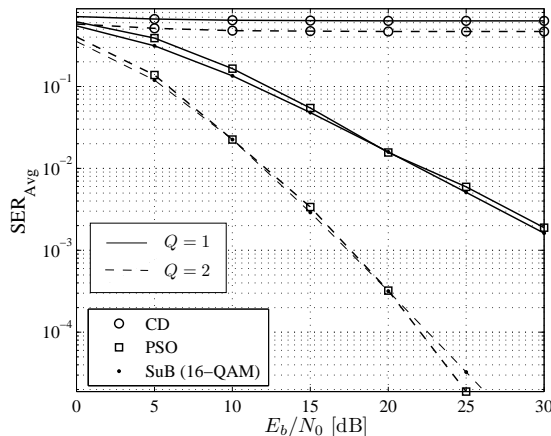


Fig. 5. Average  $SER \times E_b/N_0$  for 16-QAM,  $K = 15$ ,  $Q = 1, 2$  and flat Rayleigh channel.

However, Fig. 6 shows that the PSO-MuD for 16-QAM modulation presents a performance degradation when the system loading is higher than 50%.

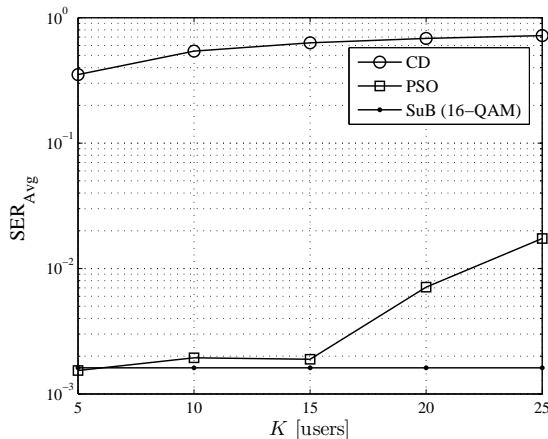


Fig. 6. PSO-MuD and CD performance degradation  $\times$  system loading under 16-QAM modulation, in flat Rayleigh channel with  $E_b/N_0 = 30$  dB.

## V. CONCLUSIONS

This paper provides an analysis of the PSO scheme applied to the multiuser DS-CDMA system with 16-QAM modulation, focusing on the parameters optimization of the algorithm, specially for the acceleration coefficients ( $\phi_1$  and  $\phi_2$ ) in Rayleigh flat channels. It was observed that  $\phi_1 = 6$  and  $\phi_2 = 1$  provide a good result (near to the optimum) for low and moderate system loading.

## REFERENCES

- [1] S. Moshavi, "Multi-user detection for ds-cdma communications," *IEEE Communication Magazine*, vol. 34, pp. 132–136, Oct. 1996.
- [2] S. Verdú, *Multiuser Detection*. New York: Cambridge University Press, 1998.
- [3] —, "Computational complexity of optimum multiuser detection," *Algorithmica*, vol. 4, no. 1, pp. 303–312, 1989.
- [4] P. Castoldi, *Multiuser Detection in CDMA Mobile Terminals*. London, UK: Artech House, 2002.
- [5] M. J. Juntti, T. Schlosser, and J. O. Lilleberg, "Genetic algorithms for multiuser detection in synchronous cdma," in *Proceedings of the IEEE International Symposium on Information Theory*, 1997, p. 492.
- [6] C. Ergün and K. Hacıoglu, "Multiuser detection using a genetic algorithm in cdma communications systems," *IEEE Transactions on Communications*, vol. 48, pp. 1374–1382, 2000.
- [7] F. Ciriaco, T. Abrão, and P. J. E. Jeszensky, "Ds/cdma multiuser detection with evolutionary algorithms," *Journal Of Universal Computer Science*, vol. 12, no. 4, pp. 450–480, 2006.
- [8] A. A. Khan, S. Bashir, M. Naeem, and S. I. Shah, "Heuristics assisted detection in high speed wireless communication systems," in *IEEE Multitopic Conference*, Dec. 2006, pp. 1–5.
- [9] H. Zhao, H. Long, and W. Wang, "Pso selection of surviving nodes in qrm detection for mimo systems," in *GLOBECOM - IEEE Global Telecommunications Conference*, Nov. 2006, pp. 1–5.
- [10] L. D. Oliveira, F. Ciriaco, T. Abrão, and P. J. E. Jeszensky, "Particle swarm and quantum particle swarm optimization applied to ds/cdma multiuser detection in flat rayleigh channels," in *ISSSTA'06 - IEEE International Symposium on Spread Spectrum Techniques and Applications*, Manaus, Brazil, 2006, pp. 133–137.
- [11] T. Abrão, L. D. de Oliveira, F. Ciriaco, B. A. Angélico, P. J. E. Jeszensky, and F. J. C. Palacio, "S/mimo mc-cdma heuristic multiuser detectors based on single-objective optimization," *Wireless Personal Communications*, April 2009.
- [12] H. S. Lim and B. Venkatesh, "An efficient local search heuristics for asynchronous multiuser detection," *IEEE Communications Letters*, vol. 7, no. 6, pp. 299–301, June 2003.
- [13] L. D. Oliveira, F. Ciriaco, T. Abrão, and P. J. E. Jeszensky, "Local search multiuser detection," *AEÜ International Journal of Electronics and Communications*, vol. 63, no. 4, pp. 259–270, April 2009.
- [14] L. D. Oliveira, T. Abrão, P. J. E. Jeszensky, and F. Casadevall, "Particle swarm optimization assisted multiuser detector for m-qam ds/cdma systems," in *SIS'08 - IEEE Swarm Intelligence Symposium*, Sept. 2008, pp. 1–8.
- [15] S. K. K., S. Y. M., C. W. S., Y. L., and C. R. S., "Particle-swarm-optimization-based multiuser detector for cdma communications," *IEEE transactions on Vehicular Technology*, vol. 56, no. 5, pp. 3006–3013, May 2007.
- [16] J. Proakis, *Digital Communications*. McGraw-Hill, McGraw-Hill, 1989.
- [17] J. Kennedy and R. Eberhart, "A discrete binary version of the particle swarm algorithm," in *IEEE international conference on Systems*, 1997, pp. 4104–4108.
- [18] R. Eberhart and Y. Shi, "Particle swarm optimization: developments, applications and resources," in *Proceedings of the 2001 Congress on Evolutionary Computation*, vol. 1, May 2001, pp. 81–86.
- [19] Y. Shi and R. C. Eberhart, "Parameter selection in particle swarm optimization," in *1998 Annual Conference on Evolutionary Programming*, San Diego, USA, March 1998.